DALTON

Photoluminescent cyclometallated diplatinum(II,II) complexes: photophysical properties and crystal structures of $[PtL(PPh_3)]ClO_4$ and $[Pt_2L_2(\mu\text{-dppm})][ClO_4]_2$ (HL = 6-phenyl-2,2′-bipyridine, dppm = $Ph_2PCH_2PPh_2$)

Tsz-Chun Cheung,[a] Kung-Kai Cheung,[a] Shie-Ming Peng[b] and Chi-Ming Che*[,a]

[a] *Department of Chemistry, The University of Hong Kong, Pokfulam Road, Hong Kong*
[b] *Department of Chemistry, National Taiwan University, Taipei, Taiwan*

The complexes [PtL(Cl)] **1**, $[PtL(PPh_3)]ClO_4$ **2** and $[Pt_2L_2(\mu\text{-dppm})][ClO_4]_2$ **3** (HL = 6-phenyl-2,2′-bipyridine, dppm = $Ph_2PCH_2PPh_2$) have been prepared and their spectroscopic and emission properties studied. Complex **3** shows a broad and intense absorption at 420–510 nm which is tentatively assigned to a metal–metal to ligand charge-transfer transition ^{1}m.m.l.c.t. $^1[d_{\sigma^*} \longrightarrow \sigma(\pi^*)]$, where d_{σ^*} arises from the antisymmetric combination of the two platinum d_{z^2} orbitals and $\sigma(\pi^*)$ from the symmetric combination of π^* orbitals of the two L ligands. All the complexes show luminescence in both the solid state and in solution. Both **1** and **2** display ^{3}m.l.c.t. emission in solution at room temperature. The solid-state emission of **1** and both the solid-state and fluid-state emission of **3** are assigned to the ^{3}m.m.l.c.t. $^3[(d_{\sigma^*})\{\sigma(\pi^*)\}]$ state. The crystal structure of **2** shows an intermolecular π–π interaction between two L ligands as evidenced by the intermolecular ligand plane separation of 3.35 Å. The solid-state emission of **2** is suggested to arise from a π–π excimeric interaction of the L ligands. The crystal structure of **3** shows discrete $[Pt_2L_2(\mu\text{-dppm})]^{2+}$ units with an intramolecular Pt–Pt separation of 3.2703 Å.

Square-planar d^8 transition-metal complexes are known to exhibit metal–metal bonding interaction in the solid state.[1] Such interaction between molecules stacked within a chain leads to anisotropic and characteristic spectral properties. Luminescent platinum(II) complexes such as $[Pt(\alpha\text{-diimine})X_2]$ (X = halide or cyanide) and $[Pt(\alpha\text{-diimine})_2]^{2+}$ have revealed a remarkable variety of low-energy excited states.[2–4] As suggested by Miskowski and co-workers[2] and others,[3] these include the α-diimine intraligand states of both the monomer (π–π*) and 'excimer' $\sigma^*(\pi) \longrightarrow \sigma(\pi^*)$, and oligomer metal–metal to ligand charge-transfer $d_{\sigma^*}(d_{z^2}) \longrightarrow \sigma(\pi^*)$ m.m.l.c.t. and monomer ligand–field (l.f.) states. Although this class of α-diimine platinum(II) complexes have intriguing photophysical properties, most often they are not good emitters or even non-emissive in the fluid state. Since square-planar d^8 complexes are unstable with respect to a D_{2d} distortion,[5] this is likely to facilitate non-radiative decay.[6] In the course of finding new luminescent metal complexes with co-ordinative unsaturated excited states in solution, we studied complexes of the type [PtL(X)] where L denotes *o*-C-deprotonated 6-phenyl-2,2′-bipyridine. There are several reasons for choosing this system: (1) the ligand shows a strong preference for planar geometry and can therefore be expected to discourage the D_{2d} distortion which promotes radiationless decay; (2) the extended π system within the ligand and the strong σ-donating power of the deprotonated carbon donor would increase the energy difference between the metal-centred d–d state and the metal-to-ligand charge-transfer (m.l.c.t.) states. [Cyclometallated platinum(II) complexes are known to have low-lying m.l.c.t. states with useful photochemical and photophysical properties [7]]; (3) the ability to vary the X group affords the possibility of having a series of related complexes with tunable photophysical properties. Herein we describe the photophysical properties of platinum(II) complexes derived from [PtL(X)]. The complex $[Pt_2L_2(\mu\text{-dppm})]^{2+}$ [dppm = bis(diphenylphosphino)methane] features an interesting model for study of the absorption and emission properties of cyclometallated platinum(II) complexes.

Experimental

Materials

The chemicals $Ph_2PCH_2PPh_2$ (dppm), PPh_3, $K_2[PtCl_4]$ and $LiClO_4$ were obtained from Aldrich Chemical Co. 6-Phenyl-2,2′-bipyridine (HL) was prepared by modification of the literature method.[8] The organic solvents for spectroscopic work were analytical grade and were purified by standard procedures before use.[9]

Preparations

[PtL(Cl)] 1. A modification of Constable's method was used.[10] A mixture of $K_2[PtCl_4]$ (200 mg, 0.48 mmol) and 6-phenyl-2,2′-bipyridine (112 mg, 0.48 mmol) in MeCN–water (15 cm^3:15 cm^3) was refluxed for 18 h to give a deep red solution. This was evaporated to dryness and the product extracted with dichloromethane. The volume of the extract was reduced to *ca.* 5 cm^3. Upon addition of diethyl ether the [PtL(Cl)] complex was obtained as an orange solid. It was purified by slow evaporation of the MeCN solution. Yield 80% (Found: C, 34.70; H, 2.50; N, 6.60. Calc. for $C_{16}H_{11}ClN_2Pt$: C, 34.85; H, 2.70; N, 6.75%). FAB mass spectrum: *m/z* 461 (M^+). ^{1}H NMR (CD_2Cl_2, 270 MHz): δ 7.05–7.11 (m, 1 H), 7.15–7.24 (m, 1 H), 7.32–7.35 (m, 1 H), 7.44–7.68 (m, 4 H), 7.79–7.85 (m, 1 H), 7.89–7.92 (m, 1 H), 8.02–8.09 (ddd, 1 H) and 8.94–9.01 (m, 1 H).

$[PtL(PPh_3)]ClO_4$ 2. To a solution of complex **1** (100 mg, 0.217 mmol) in acetonitrile (20 cm^3) was added PPh_3 (57 mg, 0.217 mmol) with stirring. A clear yellow solution was obtained and solid $NaClO_4$ (0.2 g, 160 mmol) was added. The mixture was stirred at room temperature for 5 h, then filtered and evaporated to a small volume. Addition of diethyl ether gave a bright yellow solid which was filtered off and washed with diethyl ether. It was purified by vapour diffusion of diethyl ether into an MeCN solution. Yield 85% (Found: C, 51.70; H, 3.25; N, 3.45. Calc. for $C_{34}H_{26}ClN_2O_4PPt$: C, 51.80; H, 3.35; N, 3.55%). FAB mass spectrum: *m/z* 688 (M^+).

$[Pt_2L_2(\mu\text{-dppm})][ClO_4]_2$ 3. A mixture of complex **1** (150 mg, 0.32 mmol) and dppm (62 mg, 0.16 mmol) in MeCN–MeOH (15 cm^3:15 cm^3) was stirred for 12 h under a nitrogen atmosphere, then filtered and evaporated to small volume. Addition of an excess of $LiClO_4$ gave a bright orange solid, which was filtered off and washed with water and diethyl ether. The crude product was recrystallized by vapour diffusion of diethyl ether into an acetonitrile solution. Yield 80% (Found: C, 47.60; H, 2.95; N, 3.85. Calc. for $C_{57}H_{44}Cl_2N_4O_8P_2Pt_2$: C, 47.70; H, 3.10; N, 3.90%). FAB mass spectrum: m/z 1337 (M^+). NMR: $^{31}P\text{-}\{^1H\}$ (MeCN), δ 20.35, ^1J(PtP) 2083; ^1H (CD_3CN, 270 MHz), δ 4.86 [t, CH_2, $^3J(PtPCH_2)$ = 12.9 Hz], 6.16–6.18 (m, 2 H), 6.41–6.52 (m, 4 H), 6.66–6.72 (m, 4 H), 6.93–6.97 (m, 2 H) and 7.44–8.01 (m, 30 H).

Physical measurements and instrumentation

Proton and ^{31}P NMR spectra were recorded on JEOL 270 multinuclear FT-NMR spectrometers with chemical shifts (δ) relative to tetramethylsilane (^1H) and external H_3PO_4 (^{31}P), UV/VIS spectra on a Milton Roy Spectronic 3000 array spectrometer and steady-state emission spectra on a SPEX Fluorolog-2 spectrofluorometer. Emission lifetime measurements were performed with a Quanta Ray DCR-3 Nd-YAG laser (pulsed output 355 nm, 8 ns). The decay signal was recorded by an R928 photomultiplier tube (Hamamatsu) digitized with a Tektronix 2430 digital oscilloscope interfaced to an IBM PC/AT computer, equipped with single-exponential fitting. Solutions for photochemical experiments were degassed by at least four freeze–pump–thaw cycles.

Crystallography

Crystal data. *Complex* **2**. $C_{34}H_{26}ClN_2O_4PPt$, M_r = 788.11, triclinic, space group $P\bar{1}$ (no. 2), a = 9.665(3), b = 16.585(3), c = 9.224(1) Å, α = 91.43(1), β = 92.18(2), γ = 90.05(2)°, U = 1477.0(5) $Å^3$, Z = 2, D_c = 1.772 g cm^{-3}, μ(Mo-Kα) = 49.18 cm^{-1}, $F(000)$ = 772.

Complex **3**. $C_{57}H_{44}Cl_2N_4O_8P_2Pt_2$, M_r = 1436.02, monoclinic, space group $P2/n$, a = 12.716(2), b = 15.007(2), c = 13.471(3) Å, β = 94.37(2)°, U = 2563.4(8) $Å^3$, Z = 2, D_c = 1.861 g cm^{-3}, μ(Mo-Kα) = 57.57 cm^{-1}, $F(000)$ = 1390.

For complex **2** a crystal of dimensions 0.20 × 0.15 × 0.35 mm was used for data collection at 25 °C on a Rigaku AFC7R diffractometer with graphite-monochromated Mo-Kα radiation (λ = 0.710 73) using ω–2θ scans with ω-scan angle (0.73 + 0.35 tan θ)° at a scan speed of 16.0° min^{-1} [up to four scans for reflections having $I < 15\sigma(I)$]. Intensity data ($2\theta_{max}$ = 45°, h 0–10, k −17 to 17, l −9 to 9) were corrected for decay and Lorentz-polarization effects. Upon averaging the 4128 reflections, 3854 of which were unique (R_{int} = 0.036), 2687 with $I > 3\sigma(I)$ were considered observed and used in the structural analysis.

The space group being centric was confirmed by the successful refinement of the structure which was solved by heavy-atom Patterson methods and expanded using Fourier techniques.[11] Refinement was by full-matrix least squares using TEXSAN [12a] on a SiliconGraphic Indy computer. The 43 non-H atoms were refined anisotropically, and the 26 H atoms at calculated positions with thermal parameters equal to 1.3 times that of the attached C atoms were not refined. Convergence for 388 parameters by least-squares refinement on F with $w = 4F_o^2/\sigma^2(F_o^2)$, where $\sigma^2(F_o^2) = [\sigma^2(I) + (0.03F_o^2)^2]$ for 2687 reflections with $I > 3\sigma(I)$, was reached at R = 0.037 and R' = 0.047 with a goodness of fit of 1.46; $(\Delta/\sigma)_{max}$ = 0.01. The final Fourier-difference map was featureless, with maximum positive and negative peaks of 1.20 and 0.75 e $Å^{-3}$ respectively. Final atomic coordinates are given in Table 5.

For complex **3** a crystal of dimensions 0.15 × 0.40 × 0.50 mm was used for data collection at 25 °C on a Nonius diffractometer with graphite-monochromated Mo-Kα radiation (λ = 0.7107 Å) using ω–2θ scans with ω-scan angle 2(0.80 + 0.35 tan θ)° at a scan speed of 2.06–5.50° min^{-1}. Intensity data ($2\theta_{max}$ = 50°, h −15 to 15, k 0–17, l 0–15) were corrected for decay and Lorentz and polarization effects and an empirical absorption correction was made. 4504 Reflections were uniquely measured of which 3594 with $I > 2\sigma(I)$ were considered observed and used in the structural analysis. The structure was solved and expanded as for that of **2** and refined by full-matrix least squares using the NRCVAX program.[12b] The C/N assignment was based on the thermal parameters and R values. Convergence for 350 parameters by least-squares refinement as for **2** for 3594 reflections with $I > 2\sigma(I)$ was reached at R = 0.033 and R' = 0.032 with a goodness of fit of 2.14; $(\Delta/\sigma)_{max}$ = 0.019. The final Fourier-difference map was featureless, with maximum positive and negative peaks of 2.01 and 1.24 e $Å^{-3}$ respectively. One of the perchlorate ions was disordered and atoms O(3)–O(5) have occupancy 2/3. Final atomic coordinates are given in Table 6.

Complete atomic coordinates, thermal parameters, and bond lengths and angles have been deposited at the Cambridge Crystallographic Data Centre. See Instructions for Authors, *J. Chem. Soc., Dalton Trans.*, 1996, Issue 1.

Results and Discussion

Constable *et al.*[10] previously reported that the reaction of $K_2[PtCl_4]$ with 6-phenyl-2,2′-bipyridine in MeCN–water gave [PtL(Cl)] **1**, which underwent solvolysis in acetonitrile to $[PtL(MeCN)]PF_6$. The crystal structure of $[PtL(MeCN)]^+$ was reported.[10b] The cations formed discrete dimeric units with short Pt · · · Pt contacts of 3.28(1) Å.

In this work complex **1** was prepared by a modification of the previous method.[10] The substitutional lability of the co-ordinated chloride allows easy modification of the structure and electronic properties of the complex. The complex cations $[PtL(PPh_3)]^+$ **2** and $[Pt_2L_2(\mu\text{-dppm})]^{2+}$ **3** were obtained by treating **1** with the corresponding phosphine ligands in acetonitrile. The $^{31}P\text{-}\{^1H\}$ NMR spectrum of **3** was consistent with its formula as only a central peak with two ^{195}Pt satellites was observed.

Fig. 1(*a*) shows a perspective view of complex **2** and selected bond parameters are given in Table 1. The co-ordination geometry of the Pt atom is slightly distorted square planar with the N(2)–Pt–C(1) angle of 157.9(4)° deviating from linearity. The bond distances and angles are comparable to those found in $[PtL(MeCN)]^+$. One special feature of the crystal lattice, shown in Fig. 1(*b*), is the intermolecular plane separation of 3.35 Å, suggesting the existence of weak π–π interaction between two L ligands. There is no close Pt · · · Pt interaction between adjacent complexes (Pt · · · Pt > 4 Å). This is attributed to the bulky PPh_3 ligand, which hinders approach of the two platinum centres. As discussed later, the weak π–π interaction leads to intriguing solid-state emission.

Fig. 2 shows a perspective view of complex **3** and selected bond parameters are given in Table 2. The complex consists of two PtL units bridged by a dppm ligand. The two planar PtL units are staggered with a torsion angle of 44.6°, and their configurations are identical, being related by a C_2 axis passing through the CH_2 unit of the dppm ligand. The co-ordination geometries of the two Pt atoms are slightly distorted square planar. The mean deviation of the Pt atom from the ligand plane is 0.0470 Å and the N(1)–Pt(1)–N(2) angle of 76.9(2)° and N(2)–Pt(1)–C(16) angle of 80.5(3)° significantly deviate from 90°. The two PtL units are nearly parallel to each other as suggested by the dihedral angle of about 6.1°. The intramolecular Pt–Pt distance of 3.2703 Å is somewhat longer than that of $[Pt_2(NH_3)_4(\mu\text{-}C_4H_5N_2O_2)_2]^{2+}$ (3.131 Å)[13] and $[Pt_2(terpy)_2(Gua)]^{3+}$ (terpy = 2,2′:6′,2″-terpyridine, Gua = guaninate) (3.090 and 3.071 Å)[14] but shorter than that found in $[Pt_2(dppm)_2(CN)_4]$ (3.301 Å)[15] and $[Pt_2(terpy)_2(\mu\text{-pz})]^{3+}$

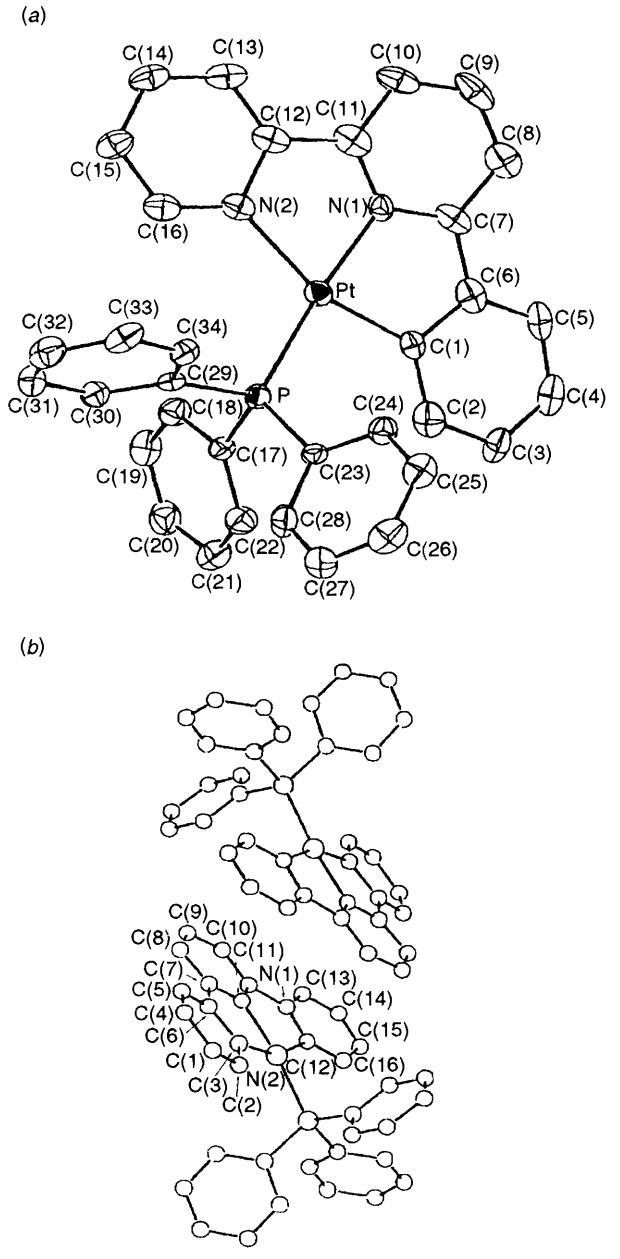

Fig. 1 (*a*) A perspective view of the $[PtL(PPh_3)]^+$ cation. (*b*) Crystal-packing diagram showing a pair of π–π interacting $[PtL(PPh_3)]^+$ cations

Table 1 Selected bond distances (Å) and angles (°) for complex **2**

Pt–P	2.243(3)	Pt–N(2)	2.12(1)
Pt–N(1)	1.985(1)	Pt–C(1)	2.00(1)
C(1)–C(6)	1.40(2)	C(1)–C(2)	1.40(2)
N(2)–C(16)	1.34(2)	N(2)–C(12)	1.37(1)
N(1)–C(7)	1.35(2)	N(1)–C(11)	1.33(2)
P–Pt–N(1)	173.8(3)	P–Pt–N(2)	105.4(3)
P–Pt–C(1)	96.3(4)	N(1)–Pt–N(2)	78.1(4)
N(1)–Pt–C(1)	80.6(5)	N(2)–Pt–C(1)	157.9(4)

(pz = pyrazolate) (3.432 Å).[16] It is also comparable to the intermolecular Pt ••• Pt separation of 3.345(2) Å in the crystal lattice of **1**[17] and of 3.381 Å in $K_2[Pt(CN)_4]\cdot 3H_2O$.[18] In square-planar platinum(II) complexes consisting of monomeric units stacked to form a continuous chain of metal atoms the intermolecular Pt ••• Pt distances lie in the range 3.09–3.50 Å.[1a]

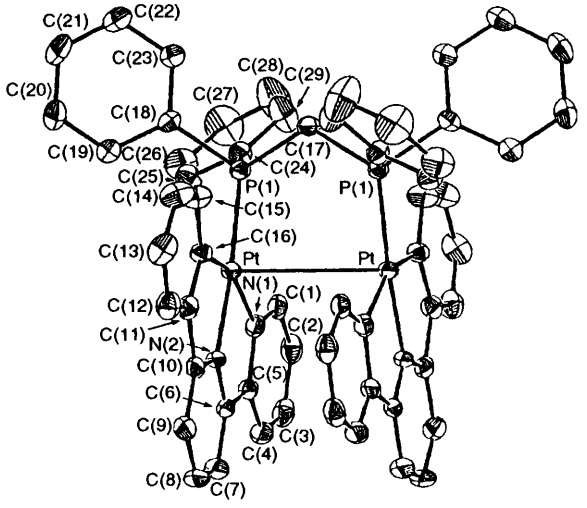

Fig. 2 Perspective view of the $[Pt_2L_2(\mu\text{-dppm})]^{2+}$ cation

Table 2 Selected bond distances (Å) and angles (°) for complex **3**

Pt–Pt	3.2703(9)	Pt–P(1)	2.248(2)
Pt–N(1)	2.160(6)	Pt–N(2)	2.006(6)
Pt–C(16)	2.024(7)	P(1)–C(17)	1.851(5)
P(1)–C(18)	1.823(7)	P(1)–C(24)	1.831(7)
N(1)–C(1)	1.335(9)	N(1)–C(5)	1.354(1)
N(2)–C(6)	1.329(1)	N(2)–C(10)	1.368(9)
Pt–Pt–P(1)	85.84(4)	Pt–Pt–N(1)	79.1(1)
Pt–Pt–N(2)	98.1(2)	Pt–Pt–C(16)	104.6(2)
P(1)–Pt–N(1)	106.1(2)	P(1)–Pt–N(2)	175.5(2)
P(1)–Pt–C(16)	96.4(2)	N(1)–Pt–N(2)	76.9(2)
N(1)–Pt–C(16)	157.4(3)	N(2)–Pt–C(16)	80.5(3)
Pt–P(1)–C(17)	116.1(3)	Pt–P(1)–C(18)	113.9(2)
Pt–P(1)–C(24)	117.2(3)		

In the present structure there is no close intermolecular Pt ••• Pt interaction between adjacent $[Pt_2L_2(\mu\text{-dppm})]^{2+}$ molecules.

An interesting structural feature of complex **3** is the large torsion angle of 44.6° between the two PtL moieties. To achieve maximum overlap of orbitals the two Pt atoms should be arranged in a face-to-face manner and the overall effect is to make the complex eclipsed. However, the π–π repulsive interaction between the two L ligands would not favour an eclipsed geometry. We attribute the large torsion angle mainly to the π–π interaction of the two L ligands in the PtL units.

Absorption and emission properties

The absorption spectra of complexes **1** and **2** are depicted in Fig. 3 and the spectral data are listed in Table 3. For **1** there are several intense transitions in the range 250–370 nm, which are tentatively assigned to the intraligand transitions of the L ligand. The broad absorption at 400–445 nm is too low in energy to be the intraligand π–π* and is too intense (ε 1550–1020 $dm^3\ mol^{-1}\ cm^{-1}$) to be a d–d transition. Most likely it is due to the m.l.c.t. transition, Pt ⟶ π*(L), analogous to those identified in the spectra of platinum(II) complexes of 2,2′-bipyridine and 2,2′:6′,2″-terpyridine.[2c,3c] Not surprisingly, this low-energy absorption shows solvatochromism in different solvents as illustrated by the absorption spectra shown in the inset of Fig. 3. The absorption tail at 450–500 nm (ε 900–200 $dm^3\ mol^{-1}\ cm^{-1}$) is tentatively assigned to the ^{3}m.l.c.t. transition.

Although the absorption profile of complex **2** is similar to that of **1**, the absorption coefficients at 405–460 nm are low (ε 980–300 $dm^3\ mol^{-1}\ cm^{-1}$). Presumably, the higher electronic

Table 3 The UV/VIS spectral data for [PtL(Cl)] **1**, [PtL(PPh_3)]ClO_4 **2** and [Pt_2L_2(μ-dppm)][ClO_4]$_2$ **3** in acetonitrile at room temperature

Complex	λ/nm (ε/dm^3 mol^{-1})
1	275 (19 600), 330 (900), 360 (5000), 400–445 (1550–1020), 450–500 (900–200)
2	266 (24 000), 336 (11 200), 350 (10 700), 375–402 (2480–1020), 405–460 (980-300)
3	< 305 (> 10^5), 340 (16 500), 420 (3900), 478 (2550), 504 (1670)

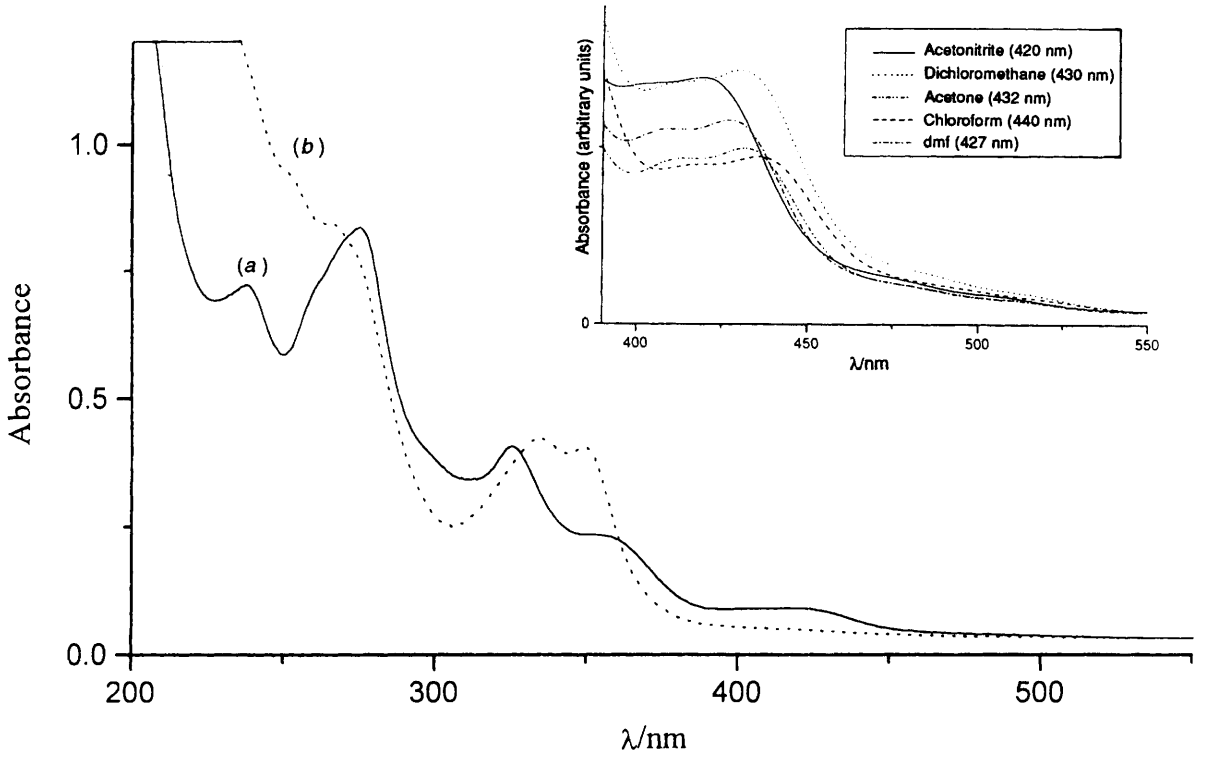

Fig. 3 Room-temperature absorption spectra of (*a*) [PtL(Cl)] (4.2 × 10^{-5} mol dm^{-3}) and (*b*) [PtL(PPh_3)]ClO_4 (3.8 × 10^{-5}mol dm^{-3}) measured in MeCN. Inset shows the solvent effect on the m.l.c.t. absorption of [PtL(Cl)]

charge of the former complex results in the m.l.c.t. transition occurring at a higher energy.

The absorption spectrum of complex **3** is shown in Fig. 4. There is a low-energy band at λ = 420 nm (ε = 3900 dm^3 mol^{-1} cm^{-1}) with two shoulders at 478 (ε = 2550) and 504 nm (ε = 1670 dm^3 mol^{-1} cm^{-1}). It should be noted that [PtL(Cl)] has a much lower molar absorption coefficient at 420–510 nm. According to previous studies,[2b,14,16] both metal–metal and ligand–ligand interactions exist in dinuclear platinum(II) complexes of aromatic diimines. These interactions could give rise to a number of electronic transitions. A simplified molecular-orbital diagram according to the work of Miskowski and Houlding[2b] is given in Fig. 5. According to the results of extended-Hückel molecular-orbital (EHMO) calculations,† the d_{σ^*} and σ*(π) orbitals are very close in energy and the lowest unoccupied MO is the σ(π*) from the two interacting L ligands. Thus the low-energy absorptions at 420–510 nm are tentatively assigned to metal–metal to ligand charge-transfer

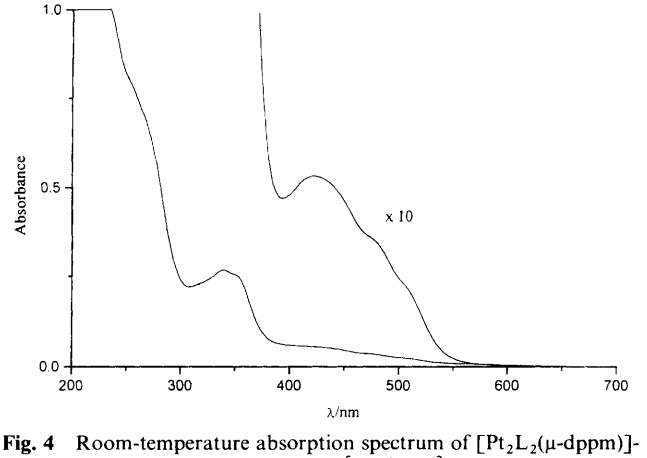

Fig. 4 Room-temperature absorption spectrum of [Pt_2L_2(μ-dppm)][ClO_4]$_2$ measured in MeCN (9 × 10^{-5} mol dm^{-3})

^{1}m.m.l.c.t. $^1[d_{\sigma^*} \longrightarrow \sigma(\pi^*)]$ and intraligand $^1[\sigma^*(\pi) \longrightarrow \sigma(\pi^*)]$ transitions. Similar ^{1}m.m.l.c.t. transitions have previously been reported in [Pt_2(terpy)$_2$(Gua)]$^{3+}$ [3c] and in [Pt_2(terpy)$_2$(μ-pz)]$^{3+}$.[16] It should be noted that all the above-mentioned absorption bands obey the Beer law in the concentration range of 10^{-6}–10^{-3} mol dm^{-3} suggesting no dimerization or oligomerization of the metal complex.

All the complexes studied in this work are highly emissive in the solid state and in solution. The solvent effect on the emission of complex **1** at a concentration of ≈10^{-6} mol dm^{-3} has been studied and its emission spectra measured at room temperature and at 77 K are shown in Fig. 6. There is no

† For complex **3** the four frontier occupied molecular orbitals are very similar in energy. Owing to the large torsion angle (44.6°) between the two PtL moieties, the five d orbitals of the Pt atoms mix substantially. According to the calculation, the first and second highest occupied MOs are the d_{δ^*} and d_{δ} which come from the bonding and antibonding interaction obtained upon mixing of the d_{xy} and $d_{x^2-y^2}$ orbitals of the two Pt atoms respectively. The third is the d_{σ^*} which comes from the antibonding interaction of the two Pt d_{z^2} orbitals. The fourth HOMO is σ*(π) formed by bonding interaction of the π orbitals of the two L ligands. The d_{δ^*}, d_{δ}, d_{σ^*} and σ*(π) orbitals are very similar in energy [the difference between the d_{δ^*} and σ*(π) orbitals is 0.11 eV, *ca.* 1.76 × 10^{-20} J]. The LUMO is σ*(π*) formed by the antibonding interaction of the π* orbitals in the face-to-face L ligands.

significant change in emission energy from CH_2Cl_2 to MeCN but the emission lifetime and quantum yield decrease as the solvent polarity increases.

However, in the frozen state at 77 K (concentration $\approx 10^{-6}$ mol dm^{-3}) the emission of complex **1** shows a large solvatochromism shift. The emission maximum changes from 512 nm in MeCN to 567 nm in CH_2Cl_2 (Table 4). The emission shows well resolved vibronic structure and the vibronic progression is in the range $\approx 1200\ cm^{-1}$, which is assigned to the skeletal stretching of the L ligand. Owing to the low complex concentration used in the measurements, the formation of an excimer and interacting dimer are precluded. The remarkable solvatochromism of the emission and the highly vibronic emission profile suggest that the emission is ^{3}m.l.c.t. in nature.

In contrast to the glass emission, the emission from a microcrystalline sample is lower in energy. The solid-state emission spectrum measured at room temperature shows a peak centred at 665 nm and a shoulder at 698 nm. At 77 K the band width of the emission reduces and the emission maximum shifts to 700 nm. The large difference in energy between the solid-state and the MeCN glassy emissions indicates different electronic origins of the emitting states.

An important problem in understanding the nature of the excited state in stacked platinum(II) complexes is its localization in the extended structure. Yersin and Gliemann[19] suggested that the excited state of the stacked $[Pt(CN)_4]^{2-}$ complex is highly localized in several molecules. In the present case, the solid-state emission of **1** probably comes from an excited state involving metal–metal interaction. In order to have a better understanding of this kind of solid-state effect the photophysical and spectroscopic properties of complex **3**, which serves as a model for two interacting PtL(Cl) units, have been studied.

Both the solid state and a degassed acetonitrile solution of complex **3** are emissive. Fig. 7(*a*) shows the room-temperature emission spectrum measured with a microcrystalline sample. The emission is composed of a broad band centred around 630 nm, with a lifetime of 1.6 μs at room temperature. At 77 K the bandwidth of the emission reduces and the emission maximum shifts to 640 nm with a shoulder at 695 nm. The emission lifetime increases to 3.8 μs. The overall spectral profile of the emission is unsymmetric and is similar to that of the solid-state emission of $[Pt_2(terpy)_2(Gua)]^{3+}$ [3c] and of the red form of $[Pt(bipy)(CN)_2]$ (bipy = 2,2′-bipyridine) and $[Pt(bipy)_2][Pt(CN)_4]$.[2a,b]

In a degassed acetonitrile solution similar emission at 652 nm with a shoulder at *ca.* 695 nm has been found [Fig. 7(*b*)]. The emission quantum yield and lifetime are 0.015 and 0.14 μs respectively. Since this emission has similar energy to that of the solid-state emission the emitting states in the two cases are likely to have the same electronic origin. Thus in the solid state the emission of complex **3** probably arises from a discrete

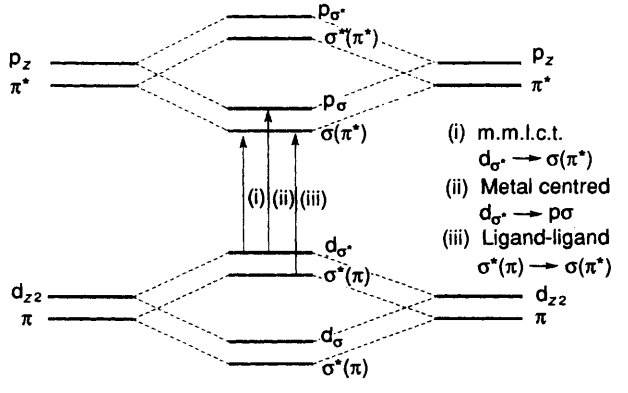

Fig. 5 Simplified schematic molecular-orbital diagram of platinum(II) complexes of polypyridine ligands with metal–metal and ligand–ligand interaction

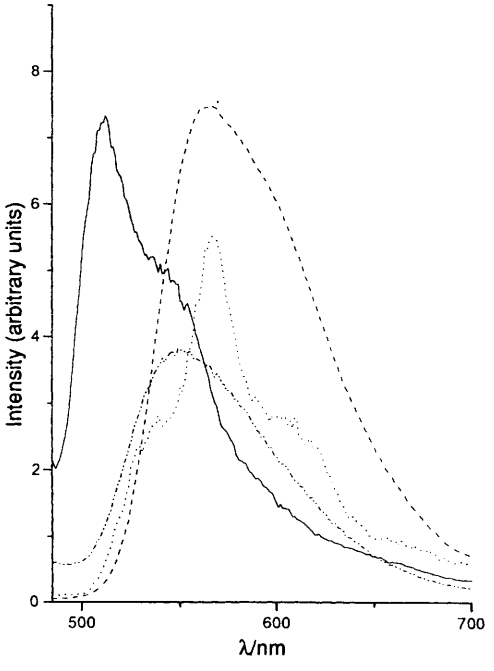

Fig. 6 Emission spectra of [PtL(Cl)] **1** in MeCN (298K) (- · · -), CH_2Cl_2 (298K) (- - -), MeCN (77 K) (——) and CH_2Cl_2 (77 K) (· · · ·)

Table 4 Photophysical data for complex **1**

	Emission			
		298 K		
Solvent	77 K λ_{max}/nm	λ_{max}/nm	Lifetime,[a] τ/μs	Quantum yield,[a] φ
Dichloromethane	535 567(max.) 610	565	0.51	0.025
Acetone	527(max.) 536	564	0.22	0.018
Chloroform	567(max.) 610	563	0.28	0.012
Acetonitrile	512(max.) 544	550	0.21	0.002
Dimethylformamide[b] (dmf)	528 560 600			

[a] Lifetimes and quantum yields measured for 1×10^{-5} mol dm^{-3} solutions. [b] Complex **1** is not emissive in dmf solution at room temperature.

Table 5 Fractional atomic coordinates for non-hydrogen atoms of complex **2** with estimated standard deviations (e.s.d.s) in parentheses

Atom	*x*	*y*	*z*	Atom	*x*	*y*	*z*
Pt	0.628 83(5)	0.308 29(3)	0.432 16(5)	C(14)	0.883(2)	0.549 1(8)	0.613(2)
Cl	0.854 9(4)	0.360 9(2)	0.074 6(4)	C(15)	0.914(1)	0.478 0(9)	0.677(1)
P	0.729 0(3)	0.196 9(2)	0.520 7(3)	C(16)	0.846(1)	0.408 0(8)	0.627(1)
O(1)	0.957(2)	0.376(1)	−0.018(2)	C(17)	0.629(1)	0.154 6(7)	0.664(1)
O(2)	0.907(1)	0.315(1)	0.177(2)	C(18)	0.597(1)	0.205 9(8)	0.778(1)
O(3)	0.738(2)	0.326 0(9)	0.015(2)	C(19)	0.520(1)	0.177 7(9)	0.891(1)
O(4)	0.817(1)	0.436(1)	0.129(2)	C(20)	0.472(1)	0.101 6(10)	0.888(1)
N(1)	0.543(1)	0.401 5(7)	0.333(1)	C(21)	0.502(2)	0.050 6(9)	0.771(2)
N(2)	0.750(1)	0.406 1(6)	0.520(1)	C(22)	0.579(1)	0.076 7(8)	0.662(1)
C(1)	0.468(1)	0.252 0(8)	0.329(1)	C(23)	0.767(1)	0.120 0(6)	0.384(1)
C(2)	0.421(1)	0.172 7(9)	0.332(1)	C(24)	0.754(1)	0.136 1(8)	0.238(1)
C(3)	0.299(1)	0.144 2(9)	0.262(1)	C(25)	0.800(1)	0.080 2(9)	0.137(1)
C(4)	0.223(1)	0.198(1)	0.184(1)	C(26)	0.858(1)	0.008 6(10)	0.182(2)
C(5)	0.265(1)	0.276(1)	0.172(1)	C(27)	0.871(1)	−0.010 5(8)	0.324(2)
C(6)	0.387(1)	0.303 1(9)	0.243(1)	C(28)	0.826(1)	0.045 6(8)	0.425(1)
C(7)	0.433(1)	0.387 1(8)	0.241(1)	C(29)	0.904(1)	0.210 1(6)	0.600(1)
C(8)	0.381(1)	0.448 1(10)	0.156(1)	C(30)	0.938(1)	0.205 4(7)	0.745(1)
C(9)	0.440(2)	0.525(1)	0.173(2)	C(31)	1.071(2)	0.217 4(9)	0.796(1)
C(10)	0.548(2)	0.539 1(8)	0.272(2)	C(32)	1.171(1)	0.236 2(9)	0.702(2)
C(11)	0.601(1)	0.474 5(9)	0.349(1)	C(33)	1.140(1)	0.242 5(8)	0.555(2)
C(12)	0.716(1)	0.478 3(8)	0.459(1)	C(34)	1.006(1)	0.229 9(7)	0.507(1)
C(13)	0.783(1)	0.548 6(8)	0.506(2)				

Table 6 Fractional atomic coordinates for non-hydrogen atoms of compound **3** with e.s.d.s in parentheses

Atom	*x*	*y*	*z*	Atom	*x*	*y*	*z*
Pt	0.206 22(2)	0.157 80(2)	0.132 68(2)	C(17)	0.25	0.362 9(7)	0.25
P(1)	0.257 51(14)	0.301 12(13)	0.131 81(12)	C(18)	0.182 8(5)	0.369 3(5)	0.039 3(5)
N(1)	0.348 0(4)	0.079 4(4)	0.126 8(4)	C(19)	0.138 7(6)	0.328 3(5)	−0.047 1(5)
N(2)	0.151 5(4)	0.032 4(4)	0.125 1(3)	C(20)	0.091 3(7)	0.379 4(7)	−0.122 8(6)
C(1)	0.448 4(6)	0.107 63(5)	0.132 1(5)	C(21)	0.086 7(8)	0.470 0(7)	−0.113 3(7)
C(2)	0.531 8(6)	0.047 3(6)	0.128 7(5)	C(22)	0.130 4(8)	0.511 2(6)	−0.028 8(6)
C(3)	0.511 7(7)	−0.042 0(7)	0.121 6(5)	C(23)	0.179 4(6)	0.460 7(6)	0.046 8(5)
C(4)	0.509 1(7)	−0.070 6(5)	0.118 4(5)	C(24)	0.388 3(5)	0.324 8(5)	0.090 0(5)
C(5)	0.328 3(6)	−0.009 2(5)	0.121 4(4)	C(25)	0.409 0(6)	0.290 3(6)	−0.003 1(5)
C(6)	0.217 4(6)	−0.035 9(5)	0.120 7(4)	C(26)	0.500 3(7)	0.310 1(7)	−0.044 8(6)
C(7)	0.179 6(7)	−0.122 3(5)	0.117 8(5)	C(27)	0.573 5(7)	0.363 8(8)	0.002 7(8)
C(8)	0.072 1(7)	−0.136 6(5)	0.119 2(6)	C(28)	0.555 2(7)	0.399 7(9)	0.093 6(8)
C(9)	0.005 0(6)	−0.064 4(6)	0.121 6(5)	C(29)	0.462 2(7)	0.379 8(7)	0.138 0(6)
C(10)	0.044 9(6)	0.020 9(5)	0.125 8(4)	Cl(1)	0.75	0.849 20(23)	0.25
C(11)	−0.011 7(6)	0.104 9(5)	0.131 8(5)	Cl(2)	0.25	0.651 5(3)	0.25
C(12)	−0.121 0(6)	0.108 0(6)	0.135 2(5)	O(1)	0.656 5(5)	0.799 1(5)	0.240 3(4)
C(13)	−0.171 2(6)	0.187 8(7)	0.142 6(6)	O(2)	0.753 3(6)	0.901 9(7)	0.169 1(8)
C(14)	−0.113 0(7)	0.266 0(6)	0.147 3(6)	O(3)	0.211 5(10)	0.665(7)	0.148 0(9)
C(15)	−0.004 5(6)	0.262 9(6)	0.143 7(6)	O(4)	0.321 5(9)	0.573 6(7)	0.238 0(8)
C(16)	0.049 9(5)	0.182 4(5)	0.134 2(5)	O(5)	0.332 2(11)	0.713 1(9)	0.218 1(9)

$[Pt_2L_2(\mu\text{-dppm})]^{2+}$ cation. This is also in accordance with the crystal structure of the compound which shows no intermolecular metal–metal interaction between adjacent $[Pt_2L_2(\mu\text{-dppm})]^{2+}$ cations. We tentatively assign the excited state as $^3[(d_{\sigma^*})\{\sigma(\pi^*)\}]$ ^{3}m.m.l.c.t. in nature. As discussed above, the solid-state emission of **1** has similar energy and band shape to that of **3**, and hence is also assigned as ^{3}m.m.l.c.t. in nature. This is in line with the crystal structure of **1**, which shows interacting dimeric units and an intermolecular Pt · · · Pt separation of 3.28(1) Å.[17]

Photoexcitation of a degassed acetonitrile solution of complex **2** at 450 nm results in an emission centred at 538 nm (lifetime 8×10^{-7} s). In a frozen MeCN solution, the emission shows vibronic structure with emission maxima at 527 and 560 nm [vibronic progression: 1118 cm^{-1}, Fig. 8(*a*)]. This is similar to the emission of **1** in acetonitrile, suggesting that the emissive excited state is also ^{3}m.l.c.t. in nature.

As shown in Fig. 8(*b*), the room-temperature solid-state emission of complex **2** is significantly different. Its profile is centred at around 600 nm and is broad and unstructured. This is reminiscent of excimer emission from planar aromatic molecules. The significantly low solid-state emission energy indicates a marked effect of the crystal structure upon the electronic structure of the monomeric complex. In the present case the Pt · · · Pt distance between adjacent complexes is greater than 4 Å (no interaction). However, as discussed in the previous section, the closest separation of 3.35 Å between the two L planes would allow overlap of the π* orbitals. Therefore, we suggest that the solid-state emission of **2** comes from a classical

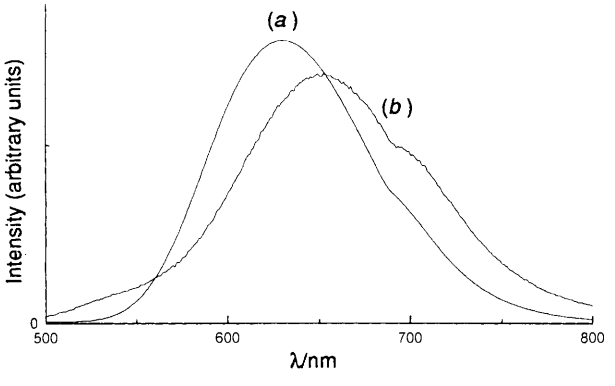

Fig. 7 Room-temperature emission spectra of $[Pt_2L_2(\mu\text{-dppm})][ClO_4]_2$: (*a*) microcrystalline sample, (*b*) MeCN solution (5×10^{-6} mol dm^{-3})

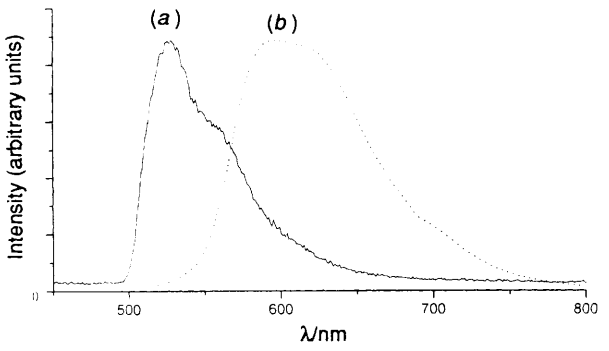

Fig. 8 (*a*) Emission spectrum of $[PtL(PPh_3)]ClO_4$ in frozen MeCN (77 K) solution (5×10^{-6} mol dm^{-3}). (*b*) Room-temperature emission spectrum of a microcrystalline sample of $[PtL(PPh_3)]ClO_4$

excimeric interaction of the L ligands. Similar excimer emission of a π-interacting dimer has been observed for $[Pt(phen)_2]Cl_2$ (phen = 1,10-phenanthroline).[2a]

Conclusion

The three complexes studied reveal interesting photoluminescent properties. The spectroscopic properties of **3** are significantly different from those of **1** and **2** and this has been rationalized in terms of the intramolecular Pt–Pt interaction in the former system. Complex **3** displays a low-energy ^{1}m.m.l.c.t. $^1[d_{\sigma^*} \longrightarrow \sigma(\pi^*)]$ transition. The spectral profile and energy of the solid-state emission of **1** are similar to those of **3**, suggesting that the emission of the stacked PtL(Cl) units is also ^{3}m.m.l.c.t. in nature. For **2** the solid-state emission occurs at low energy but this is due to excimeric π–π interaction of the L ligands.

Acknowledgements

We acknowledge support from The University of Hong Kong, the Hong Kong Research Grants Council, and the Croucher Foundation of Hong Kong.

References

1 See, for example, (*a*) J. S. Miller and A. J. Epstein, *Prog. Inorg. Chem.*, 1976, **20**, 1 and refs. therein; (*b*) *Extended Linear Chain Compounds*, ed. J. S. Miller, Plenum, New York, 1982, vols. 1–3.
2 (*a*) V. M. Miskowski and V. H. Houlding, *Inorg. Chem.*, 1989, **28**, 1529; (*b*) V. M. Miskowski and V. H. Houlding, *Inorg. Chem.*, 1991, **30**, 4446; (*c*) V. H. Houlding and V. M. Miskowski, *Coord. Chem. Rev.*, 1991, **111**, 145; (*d*) V. M. Miskowski, V. H. Houlding, C. M. Che and Y. Wang, *Inorg. Chem.*, 1993, **32**, 2518.
3 (*a*) C. M. Che, L. Y. He, C. K. Poon and T. C. W. Mak, *Inorg. Chem.*, 1989, **28**, 3081; (*b*) K. T. Wan, C. M. Che and K. C. Cho, *J. Chem. Soc., Dalton Trans.*, 1991, 1077; (*c*) H. K. Yip, L. K. Cheng, K. K. Cheung and C. M. Che, *J. Chem. Soc., Dalton Trans.*, 1993, 2933; (*d*) C. W. Chan, L. K. Cheng and C. M. Che, *Coord. Chem. Rev.*, 1994, **132**, 87.
4 J. Bidermann, G. Gilemann, U. Klement, K. J. Range and M. Zabel, *Inorg. Chem.*, 1990, **29**, 1884; H. Kunkely and A. Vogler, *J. Am. Chem. Soc.*, 1990, **112**, 5625.
5 C. J. Ballhausen, N. Bjerrum, R. Dingle, K. Eriks and C. R. Hare, *Inorg. Chem.*, 1965, **4**, 514.
6 L. J. Andrews, *J. Phys. Chem.*, 1979, **83**, 3203.
7 M. Maestri, D. Sandrini, V. Balzani, A. von Zelewsky and P. Jolliet, *Helv. Chim. Acta*, 1988, **71**, 134; M. Maestri, V. Balzani, C. Deuschel-Cornioley and A. von Zelewsky, *Adv. Photochem*, 1992, **17**, 1.
8 C. O. Dietrich-Buchecker, P. A. Marnot and J. P. Sauvage, *Tetrahedron Lett.*, 1982, **23**, 5291.
9 D. D. Perrin, W. L. F. Armarego and D. R. Perrin, *Purification of Laboratory Chemicals*, 2nd edn. Pergamon, Oxford, 1980.
10 E. C. Constable, R. P. G. Henney, T. A. Leese and D. A. Tocher, *J. Chem. Soc., Dalton Trans.*, 1990, 443; *J. Chem. Soc., Chem. Commun.*, 1990, 513.
11 PATTY & DIRDIF 92, P. T. Beurskens, G. Admiraal, G. Beurskens, W. P. Bosman, S. Garcia-Granda, R. O. Gould, J. M. M. Smits and C. Smykalla, The DIRDIF program system, Technical Report of the Crystallography Laboratory, University of Nijmegen, 1992.
12 (*a*) TEXSAN Structure Analysis Package, Molecular Structure Corporation, Houston, TX, 1985; (*b*) NRCVAX, E. J. Cabe, Y. Le Page, J. P. Charland, F. L. Lee and P. S. White, *J. Appl. Crystallogr.*, 1989, **22**, 384.
13 J. P. Laurent, P. Lepage and F. Dahan, *J. Am. Chem. Soc.*, 1982, **104**, 7335.
14 H. K. Yip, C. M. Che, Z. Y. Zhou and T. C. W. Mak, *J. Chem. Soc., Chem Commun.*, 1992, 1369.
15 C. M. Che, V. W. W. Yam, W. T. Wong and T. F. Lai, *Inorg. Chem.*, 1989, **28**, 2908.
16 J. A. Baily, V. M. Miskowski and H. B. Gray, *Inorg. Chem.*, 1993, **32**, 369.
17 C. M. Che and K. K. Cheung, unpublished work.
18 J. M. Williams, K. D. Keefer, D. M. Washecheck and N. P. Enright, *Inorg. Chem.*, 1976, **15**, 2446.
19 H. Yersin and G. Gliemann, *Struct. Bonding (Berlin)*, 1985, **66**, 87.

Received 21*st November* 1995; *Paper* 5/07599H